

Small Angle X-ray Scattering intensity of Boolean models of spheres. Supplementary materials.

LOÏC SORBIER,^{a*} MAXIME MOREAUD^{a,b} AND SÉVERINE HUMBERT^a

^a*IFP Energies nouvelles, Rond-point de l'échangeur de Solaize, BP 3, 69360 Solaize, France, and* ^b*MINES ParisTech, PSL-Research University, CMM, 35 rue Saint Honoré, 77305 Fontainebleau, France. E-mail: loic.sorbier@ifpen.fr*

1. SAXS scattered intensity

1.1. General equations

The principle of the technique is to irradiate the sample with a monochromatic X-ray beam and measure the intensity of elastically scattered X-ray in function of the scattering vector $\mathbf{q} = 2\pi(\mathbf{k} - \mathbf{k}_0)$, where \mathbf{k}_0 and \mathbf{k} are the X-ray wave vectors respectively before and after scattering. The polar angle of diffusion 2θ and \mathbf{q} are related by:

$$|\mathbf{q}| = \frac{4\pi \sin \theta}{\lambda} \quad (1)$$

with λ the X-ray wavelength. The intensity at a scattering vector \mathbf{q} is related to the electron density ρ by (Guinier *et al.*, 1955):

$$I(\mathbf{q}) = I_e(\mathbf{q}) \iiint \rho(\mathbf{r}) \rho(\mathbf{r}') e^{-i\mathbf{q} \cdot (\mathbf{r} - \mathbf{r}')} dV dV' \quad (2)$$

where $I_e(\mathbf{q})$ is the intensity scattered by a single electron (Guinier *et al.*, 1955):

$$I_e(\mathbf{q}) = I_0 \frac{r_e^2}{a^2} \frac{1 + \cos^2(2\theta)}{2} \quad (3)$$

with I_0 the intensity of incident X-ray, r_e the classical electron radius and a the distance between the electron and the detector. If electron density is constant, there is no scattering except for $\mathbf{q} = \mathbf{0}$, that is to say in the forward direction. Let $\langle f(\mathbf{r}) \rangle$ be the mathematical expectation of $f(\mathbf{r})$ on the volume V :

$$\langle f(\mathbf{r}) \rangle = \frac{1}{V} \int_V f(\mathbf{r}) \, dV \quad (4)$$

Equation 2 reads for $\mathbf{q} \neq \mathbf{0}$:

$$I(\mathbf{q}) = I_e(\mathbf{q}) \iint \Delta\rho(\mathbf{r}) \Delta\rho(\mathbf{r}') e^{-i\mathbf{q}\cdot(\mathbf{r}-\mathbf{r}')} \, dV dV' \quad (5)$$

where $\Delta\rho(\mathbf{r}) = \rho(\mathbf{r}) - \langle \rho(\mathbf{r}) \rangle$. The Debye correlation function or normalized covariance is defined by (Gommes, 2018):

$$\gamma(\mathbf{r}) = \frac{\langle \Delta\rho(\mathbf{x}) \Delta\rho(\mathbf{x} + \mathbf{r}) \rangle}{\langle \Delta\rho^2(\mathbf{x}) \rangle} \quad (6)$$

Then equation 2 writes:

$$I(\mathbf{q}) = I_e(\mathbf{q}) V \langle \Delta\rho^2(\mathbf{x}) \rangle \int_V \gamma(\mathbf{r}) e^{-i\mathbf{q}\cdot\mathbf{r}} \, dV \quad (7)$$

The SAXS intensity is proportional to the Fourier transform of the normalized covariance.

1.2. Statistically isotropic porous medium

If we assume a porous system of volume fraction p and electron density ρ in the solid phase, we have:

$$\langle \Delta\rho^2(\mathbf{x}) \rangle = p(1-p)\rho^2 \quad (8)$$

Assuming a statistically isotropic medium, the intensity depends only on $q = |\mathbf{q}|$ and the normalized covariance only on $r = |\mathbf{r}|$. We can calculate equation 7 by integration

in polar coordinates with the z axis in forward scattering direction, setting $u = \cos \theta$:

$$\begin{aligned}
 I(q) &= I_e(q) V p (1-p) \int_0^\infty \int_0^\pi \int_0^{2\pi} \gamma(r) e^{-iqr \cos \theta} r^2 \sin \theta \, d\phi \, d\theta \, dr \\
 &= I_e(q) V p (1-p) \int_0^\infty \left(2\pi r^2 \gamma(r) \int_{-1}^1 e^{-iqr u} \, du \right) \, dr \\
 &= I_e(q) V p (1-p) \int_0^\infty 4\pi r^2 \gamma(r) \frac{\sin(qr)}{qr} \, dr
 \end{aligned} \tag{9}$$

For small q , the $\text{sinc}(qr)$ term in equation 9 tends to 1 and intensity for $q = 0$ is equal to:

$$I(0) = I_e(0) V p (1-p) \rho^2 A_3 \tag{10}$$

where A_3 is the integral range (Lantuejoul, 1991) of the covariance defined by:

$$A_3 = \int_0^\infty 4\pi r^2 \gamma(r) \, dr \tag{11}$$

If $\gamma(r)$ is known, A_3 can be calculated by numerical integration as for ordinary systems, γ has either a finite support or is rapidly decreasing when r increases.

2. Computation of SAXS intensity

For the remainder of the document, microstructures are considered as defined by the electron density, a function $\rho_b : \mathbb{R}^3 \rightarrow \mathbb{R}$ with points representing matter defined by the set $X = \{\mathbf{x} \in \mathbb{R}^3 \mid \rho_b(\mathbf{x}) > 0\}$; X is a bounded set. Let $\partial\gamma$ the convex hull of X with γ a bounded set of \mathbb{R}^3 , defined as the smallest convex set such as $X \subset \gamma$. Finally let ρ be a 3D image representing the microstructure, defined by ρ_b and γ by $\rho : \gamma \rightarrow \mathbb{R}; \mathbf{x} \mapsto \rho_b(\mathbf{x})$, otherwise said ρ is a restriction of ρ_b to γ .

2.1. From analytical covariance

Defining the Fourier transform $\mathcal{F}(g)$ of g by:

$$\mathcal{F}(g)(q) = \int_{-\infty}^{+\infty} g(r) e^{-iqr} \, dr \tag{12}$$

We can rewrite equation 9:

$$I(q) = I_e(q) Vp(1-p) \rho^2 \frac{2\pi}{q} 2 \int_0^\infty r \gamma(r) \sin(qr) dr \quad (13)$$

As $\gamma(r)$ is an even function, the function $r\gamma(r)\sin(qr)$ is also even, hence:

$$I(q) = I_e(q) Vp(1-p) \rho^2 \frac{2\pi}{q} \int_{-\infty}^\infty r \gamma(r) \sin(qr) dr \quad (14)$$

As $\sin(qr) = -\Im(e^{-iqr})$, where $\Im(z)$ is the imaginary part of z and replacing r by $i(-ir)$ we obtain:

$$I(q) = I_e(q) Vp(1-p) \rho^2 \frac{-2\pi}{q} \Im \left[\int_{-\infty}^\infty i \gamma(r) (-ir) e^{-iqr} dr \right] \quad (15)$$

Noticing that $\Im(iz) = \Re(z)$ where $\Re(z)$ is the real part of z and that $(-ir)e^{-iqr} = \frac{\partial}{\partial q} [e^{-iqr}]$, we obtain:

$$\begin{aligned} I(q) &= I_e(q) Vp(1-p) \rho^2 \frac{-2\pi}{q} \Re \left[\int_{-\infty}^\infty \gamma(r) \frac{\partial}{\partial q} (e^{-iqr}) dr \right] \\ &= I_e(q) Vp(1-p) \rho^2 \frac{-2\pi}{q} \frac{\partial}{\partial q} \left[\Re \left[\int_{-\infty}^\infty \gamma(r) e^{-iqr} dr \right] \right] \end{aligned} \quad (16)$$

Identifying the Fourier transform of $\gamma(r)$ we obtain similarly to Levitz & Tchoubar (1992):

$$I(q) = I_e(q) Vp(1-p) \rho^2 \frac{-2\pi}{q} \frac{\partial}{\partial q} [\Re[\mathcal{F}(\gamma)(q)]] \quad (17)$$

Equation 17 may be helpful to compute SAXS intensity from a know covariance. It implies a one-dimensional Fourier Transform transform and a numerical differentiation. Equation 17 can be evaluated numerically by an efficient Fast Fourier Transform algorithm (FFT).

2.2. From numerical evaluation of the covariance

For random sets that do not yield to an analytical expression for the covariance, it is still possible to evaluate the covariance numerically on realizations of random sets.

For statistically isotropic porous random sets, the two-point correlation function of the solid phase $C(r)$ is related with $\gamma(r)$ by:

$$C(r) = \langle \chi(x) \chi(x+r) \rangle = p(1-p)\gamma(r) + p^2 \quad (18)$$

where χ is the indicator function of the microstructure. For periodic microstructures, the covariance may be evaluated by Fast Fourier Transform (FFT) (Koch *et al.*, 2003; Schmidt-Rohr, 2007):

$$C(\mathbf{r}) = \mathcal{F}^{-1} \left(|\mathcal{F}(\chi(\mathbf{r}))|^2 \right) \quad (19)$$

Combining equations 17 and 19, the scattered intensity writes:

$$I(q) = I_e(q) V \rho^2 \frac{-2\pi}{q} \frac{\partial}{\partial q} \left[|\mathcal{F}(\chi(\mathbf{r}))|^2 \right] \quad (20)$$

The SAXS intensity may be computed from a three-dimensional Fourier transform and a numerical differentiation.

2.3. From projection of the microstructure

Brisard *et al.* (2012) invoking the Fourier slice theorem (Kak & Slaney, 1988) indicate that the SAXS intensity is proportional to the square of the modulus of the Fourier transform of the linear projection of the microstructure. In the tomography literature (Kak & Slaney, 1988), the parallel linear projection of a function with finite support $f(\mathbf{r})$ is defined as the integral path of the function along a particular direction. For example the linear projection $\mathcal{P}_z[f]$ of $f(\mathbf{r})$ along the z axis in Cartesian coordinates is defined by:

$$\mathcal{P}_z[f](x, y) = \int_{-\infty}^{\infty} f(x, y, z) dz \quad (21)$$

Let's evaluate the intensity in the $q_z = 0$ plane. Setting $q_z = 0$ in equation 2 leads to:

$$\frac{I(q_x, q_y)}{I_e(q_x, q_y)} = \iint \rho(\mathbf{r}) \rho(\mathbf{r}') e^{-i[q_x(x-x') + q_y(y-y')]} dV dV' \quad (22)$$

As the exponential term in the integral does not depend neither on z nor on z' we can perform first the integration on z and z' :

$$\frac{I(q_x, q_y)}{I_e(q_x, q_y)} = \iint \mathcal{P}_z[\rho](x, y) \mathcal{P}_z[\rho](x', y') \times e^{-i[q_x(x-x') + q_y(y-y')]} dx dx' dy dy' \quad (23)$$

Let $\mathcal{F}(f)(q_x, q_y)$ be the two-dimensional Fourier transform of $f(x, y)$. We can rewrite equation 23 using the definition of the Fourier transform:

$$\begin{aligned} \frac{I(q_x, q_y)}{I_e(q_x, q_y)} &= \mathcal{F}(\mathcal{P}_z[\rho](x, y)) \int \mathcal{P}_z[\rho](x', y') e^{i[q_x x' + q_y y']} dx' dy' \\ &= \mathcal{F}(\mathcal{P}_z[\rho](x, y)) \mathcal{F}^*(\mathcal{P}_z[\rho](x, y)) \\ &= |\mathcal{F}(\mathcal{P}_z[\rho](x, y))|^2 \end{aligned} \quad (24)$$

The SAXS intensity in the $q_z = 0$ plane is proportional to the square modulus of the Fourier transform of the projection of the electron density along the z axis. The result is effectively obtained after applying twice the Fourier slice theorem. If we assume an isotropic medium, the scattered intensity depends only on q and may be evaluated in any direction, for example in the $q_z = 0$ plane. Notice that equation 24 may be used to evaluate the SAXS intensities of an object with continuous variation of the electron density.

Assuming a biphasic porous medium, $\rho(\mathbf{r}) = \rho\chi(\mathbf{r})$ with $\chi(\mathbf{r})$ the indicator function of the medium, equation 24 reads:

$$\frac{I(q_x, q_y)}{I_e(q_x, q_y)} = \rho^2 |\mathcal{F}(\mathcal{P}_z[\chi](x, y))|^2 \quad (25)$$

Thus, the SAXS intensity of an isotropic medium is easily calculable from the projection of the microstructure along an arbitrary direction. Only a two dimensional Fourier transform is needed.

A second projection may be performed to obtain a one-dimensional Fourier trans-

form:

$$\frac{I(q_x)}{I_e(q_x)} = \rho^2 |\mathcal{F}(\mathcal{P}_y[\mathcal{P}_z[\chi]](x))|^2 \quad (26)$$

Projecting twice is equivalent to make an average of intensities along horizontal and vertical axis for a single projection. Any type of complex yet isotropic multi-scale microstructures can be used with this approach. At last, it is not necessary to reconstruct the complete microstructure but only a linear projection of it along an arbitrary direction.

3. Validation of codes on isolated spheres

For an isolated sphere of radius R , the scattered intensity is given by (Guinier *et al.*, 1955):

$$I_S(q) = I_e(q) V_S^2 \rho^2 \left(3 \frac{\sin(qR) - qR \cos(qR)}{(qR)^3} \right)^2 \quad (27)$$

where V_S is the volume of the sphere.

The normalized covariance of an isolated sphere is equal to $K_S(R, h)/V_S$, where K_S is the geometrical covariogram:

$$\gamma_S(R, h) = \left(1 - \frac{3h}{4R} + \frac{h^3}{16R^3} \right) \Theta(2R - h) \quad (28)$$

where $\Theta(x)$ is the Heaviside's function.

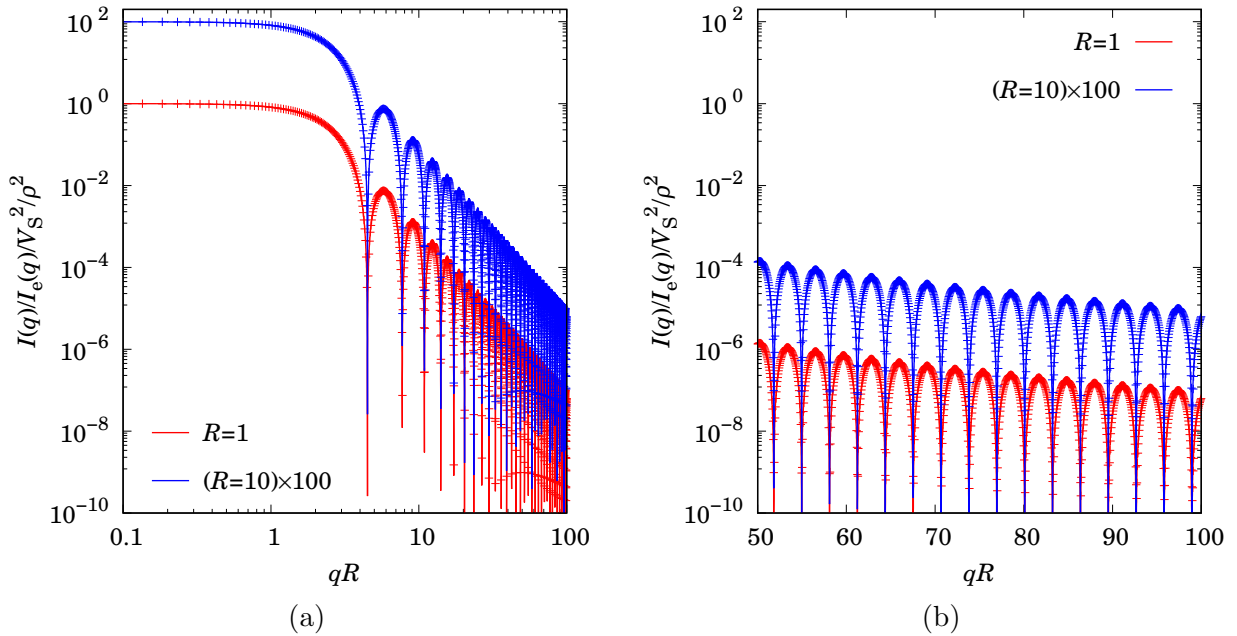


Fig. 1. Comparison of calculated SAXS intensity from analytical covariance (equation 17, symbol) with equation 27 (line) for an isolated sphere. (a) log-log plot (b) semi-log plot

Figure 1 shows the comparison of the theoretical SAXS intensity (equation 27 with the intensity computed from the covariance of an isolated sphere (equation 3). Simulation domain is 2^{18} wide and the radius of the sphere is sampled with 2^7 points. A very good agreement is found for a large range of q .

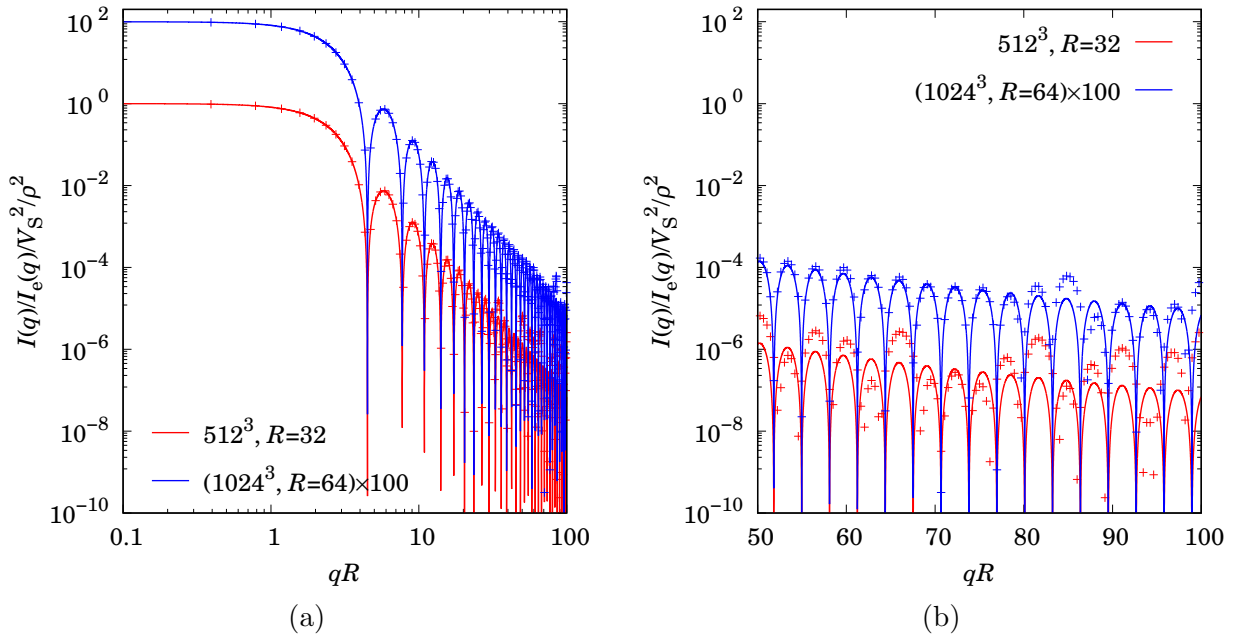


Fig. 2. Comparison of calculated SAXS intensity from projection (equation 25, symbol) with equation 27 (line) for an isolated sphere. (a) log-log plot (b) semi-log plot

Figure 2 shows the comparison of the theoretical SAXS intensity (equation 27 with the intensity computed from the projection of an isolated sphere. The size of the simulation domain and radius of the sphere is detailed in the legend of the figure. A good agreement is found for a more restricted range of q .

4. Analytical expression of covariograms for distribution in size

As a preliminary remark, the covariogram does not need to be defined in 0 as we can simply set $\gamma(0) = 1$.

4.1. Union of models with continuous radius distribution

The Choquet's capacity $T(K)$ is the probability that a compact set K is included in the random set. For a Boolean model of grain G and Poisson point intensity θ , it

is given by (Matheron, 1975):

$$T(K) = 1 - Q(K) = 1 - e^{-\theta E[V(G \oplus \check{K})]} \quad (29)$$

where \oplus denotes the Minkowski addition ($A \oplus B = \{\mathbf{a} + \mathbf{b} \mid \mathbf{a} \in A, \mathbf{b} \in B\}$), \check{K} is the symmetrical set of K with respect to the origin ($\check{K} = \{-\mathbf{x} \mid \mathbf{x} \in K\}$) and E is the expectation. Taking $K = \{\mathbf{x}\}$ as a single point, we obtain the porosity ε :

$$\varepsilon = Q(\{\mathbf{x}\}) = e^{-\theta E[V(G)]} \quad (30)$$

Taking $K = \{\mathbf{x}, \mathbf{x} + \mathbf{h}\}$ as a bi-point, we obtain the expression of the pore-pore two-points correlation function $C_{00}(h)$:

$$C_{00}(h) = Q(\{\mathbf{x}, \mathbf{x} + \mathbf{h}\}) = e^{-\theta(2E[V(G)] - E[V(G \cap G_{\mathbf{h}})])} \quad (31)$$

where $G_{\mathbf{h}}$ is G translated by a vector \mathbf{h} . The quantity $E[V(G \cap G_{\mathbf{h}})]$ is called the geometrical covariogram of the grain. For a sphere of radius R , the covariogram $K_S(R, h)$ is given by:

$$K_S(R, h) = \frac{4\pi}{3} \left(R^3 - \frac{3}{4}hR^2 + \frac{1}{16}h^3 \right) \Theta(2R - h) \quad (32)$$

and the pore-pore two-points correlation function $C_{00}(h)$ reads:

$$C_{00}(h) = \varepsilon^2 e^{\theta K_S(R, h)} \quad (33)$$

For spherical grains $G(R)$ of radius R distributed from a radius distribution $P(R)$ we have:

$$\begin{aligned} E[V(G \cap G_{\mathbf{h}})] &= \int_0^\infty E[V(G(R) \cap G_{\mathbf{h}}(R))] P(R) \, dR \\ &= \int_0^\infty P(R) K_S(R, h) \, dR \end{aligned} \quad (34)$$

The Boolean model of spheres with a radius distribution $P(R)$ behaves as a simple Boolean model with the modified covariogram:

$$K(h) = \int_0^\infty P(R) K_S(R, h) \, dR \quad (35)$$

Inserting equation 32, this covariogram reads:

$$K(h) = \frac{4\pi}{3} \left[S_P^3 \left(\frac{h}{2} \right) - \frac{3}{4} h S_P^2 \left(\frac{h}{2} \right) + \frac{1}{16} h^3 S_P^0 \left(\frac{h}{2} \right) \right] \quad (36)$$

where $S_P^n(x)$ is the uncentered partial moment of P defined by:

$$S_P^n(x) = \int_x^\infty R^n P(R) dR \quad (37)$$

4.2. Constant radius

For constant radius we have $P(r) = \delta(r - R)$ where δ is the Dirac distribution.

Then:

$$\begin{aligned} S_\delta^n(x) &= \int_x^\infty r^n \delta(r - R) dr \\ &= R^n [1 - \Theta(x - R)] \\ &= R^n \Theta(R - x) \end{aligned} \quad (38)$$

And the covariogram reads:

$$K(r, R) = \frac{4\pi}{3} \left(R^3 - \frac{3}{4} r R^2 + \frac{1}{16} r^3 \right) \Theta \left(R - \frac{r}{2} \right) \quad (39)$$

which is identical to equation 32.

4.3. Log-normal distribution

Let $L_{\mu, \sigma}(r)$ be the log-normal law of parameters $\mu \in \mathbb{R}$ and $\sigma > 0$.

$$L_{\mu, \sigma}(r) = \frac{1}{r\sigma\sqrt{2\pi}} e^{-\frac{1}{2} \left(\frac{\ln r - \mu}{\sigma} \right)^2} \quad (40)$$

For $r > 0$, setting $y = \ln r$ we have:

$$S_L^n(x) = \frac{1}{\sigma\sqrt{2\pi}} \int_{\ln x}^\infty e^{-\frac{y^2}{2\sigma^2} + (n + \frac{\mu}{\sigma^2})y - \frac{\mu^2}{2\sigma^2}} dy \quad (41)$$

After setting $z = \frac{1}{\sigma\sqrt{2}} (y - \mu - n\sigma^2)$ and $\tilde{x}_n = \frac{1}{\sigma\sqrt{2}} (\ln x - \mu - n\sigma^2)$ we obtain:

$$\begin{aligned} S_L^n(x) &= \frac{1}{\sqrt{\pi}} e^{\mu n + \frac{n^2 \sigma^2}{2}} \int_{\tilde{x}_n}^\infty e^{-z^2} dz \\ &= \frac{1}{2} e^{\mu n + \frac{n^2 \sigma^2}{2}} \operatorname{erfc}(\tilde{x}_n) \end{aligned} \quad (42)$$

Regrouping the different terms, we obtain after setting $\tilde{r}_n = \frac{1}{\sigma\sqrt{2}} (\ln \frac{r}{2} - \mu - n\sigma^2)$:

$$K(r) = \frac{2\pi}{3} \left[e^{3\mu + \frac{9\sigma^2}{2}} \operatorname{erfc}(\tilde{r}_3) - \frac{3}{4} r e^{2\mu + 2\sigma^2} \operatorname{erfc}(\tilde{r}_2) + \frac{r^3}{16} \operatorname{erfc}(\tilde{r}_0) \right] \quad (43)$$

$K(r)$ given above is not defined in $r = 0$ but does not need to be as $\gamma(0) = 1$. The mean volume-averaged radius is given by:

$$R_V = \frac{S_L^4(0)}{S_L^3(0)} = \frac{e^{4\mu + \frac{16\sigma^2}{2}}}{e^{3\mu + \frac{9\sigma^2}{2}}} = e^{\mu + \frac{7}{2}\sigma^2} \quad (44)$$

The variance $\mathcal{V}[X]$ of a random variable X reads:

$$\mathcal{V}[X] = E[X^2] - E[X]^2 \quad (45)$$

where $E[X]$ is the expected value of X . Then the variance \mathcal{V} of the volume-average radius reads:

$$\mathcal{V} = \frac{S_L^5(0)}{S_L^3(0)} - R_V^2 = e^{2\mu + 7\sigma^2} (e^{\sigma^2} - 1) \quad (46)$$

And the relative standard deviation RSD of the volume-averaged radius reads:

$$RSD = \frac{\sqrt{\mathcal{V}}}{R_V} = \sqrt{e^{\sigma^2} - 1} \quad (47)$$

The log-normal distribution allows to obtain an arbitrary large (or small) RSD for the volume-averaged radius.

4.4. Gamma distribution

Let $G_{b,c}(r)$ be the gamma distribution with scale parameter $b > 0$ and shape parameter $c > 0$:

$$G_{b,c}(r) = \left(\frac{r}{b}\right)^{c-1} \frac{e^{-\frac{r}{b}}}{b\Gamma(c)} \quad (48)$$

where $\Gamma(c)$ is the gamma function with argument c . Setting $z = r/b$ we have:

$$\begin{aligned} S_G^n(x) &= \frac{b^n}{\Gamma(c)} \int_{\frac{x}{b}}^{\infty} z^{n+c-1} e^{-z} dz \\ &= \frac{b^n}{\Gamma(c)} \Gamma\left(n+c, \frac{x}{b}\right) \end{aligned} \quad (49)$$

where $\Gamma(a, x)$ is the incomplete gamma function of arguments a and x . The covariogram reads:

$$K(r) = \frac{4\pi}{3\Gamma(c)} \left[b^3 \Gamma\left(c+3, \frac{r}{2b}\right) - \frac{3}{4} r b^2 \Gamma\left(c+2, \frac{r}{2b}\right) + \frac{r^3}{16} \Gamma\left(c, \frac{r}{2b}\right) \right] \quad (50)$$

The volume-averaged radius is given by:

$$R_V = \frac{\Gamma(c+4)}{\Gamma(c+3)} b = (c+3) b \quad (51)$$

The variance \mathcal{V} of the volume-average radius reads:

$$\begin{aligned} \mathcal{V} &= \frac{\Gamma(c+5) b^5}{\Gamma(c+3) b^3} - (c+3)^2 b^2 \\ &= \left[(c+4)(c+3) - (c+3)^2 \right] b^2 \\ &= (c+3) b^2 \end{aligned} \quad (52)$$

And the *RSD* reads:

$$RSD = \frac{1}{\sqrt{c+3}} \quad (53)$$

Keeping in mind the condition $c > 0$, it is obvious that Gamma distribution cannot lead to large *RSD* for the volume-averaged radius.

4.5. Exponential distribution

Let $E_b(r)$ be the exponential distribution with scale parameter $b > 0$:

$$E_b(r) = \frac{e^{-\frac{x}{b}}}{b} \quad (54)$$

Setting $z = r/b$ we have:

$$\begin{aligned} S_E^n(x) &= b^n \int_{\frac{x}{b}}^{\infty} z^n e^{-z} dz \\ &= b^n \Gamma\left(n+1, \frac{x}{b}\right) \end{aligned} \quad (55)$$

Using the recurrence relation $\Gamma(a+1, x) = a\Gamma(a, x) + x^a e^{-x}$ and the particular value $\Gamma(1, x) = e^{-x}$ we have:

$$S_E^0(x) = e^{-\frac{x}{b}} \quad (56)$$

$$S_E^2(x) = (x^2 + 2bx + 2b^2) e^{-\frac{x}{b}} \quad (57)$$

$$S_E^3(x) = (x^3 + 3bx^2 + 6b^2x + 6b^3) e^{-\frac{x}{b}} \quad (58)$$

The covariogram reads:

$$K(r) = \pi (2b^2r + 8b^3) e^{-\frac{r}{2b}} \quad (59)$$

which is in line with the expression given by Sonntag *et al.* (1981). The volume-averaged radius is given by:

$$R_V = \frac{\Gamma(5) b^4}{\Gamma(4) b^3} = \frac{4!}{3!} b = 4b \quad (60)$$

The variance \mathcal{V} of the volume-average radius reads:

$$\mathcal{V} = \frac{\Gamma(6) b^5}{\Gamma(4) b^3} - (4b)^2 = 4b^2 \quad (61)$$

And the *RSD* reads:

$$RSD = \frac{\sqrt{4b^2}}{4b} = \frac{1}{2} \quad (62)$$

The *RSD* of volume-averaged radius is constant and small.

5. Analytical expression of covariance for union and intersection of Boolean models

The algebra is a little simplified by the introduction of the reduced covariance $\bar{C}_{ii}(h)$ defined by:

$$\bar{C}_{00}(h) = C_{00}(h) - \varepsilon^2 = \bar{C}_{11}(h) = C_{11}(h) - p^2 \quad (63)$$

5.1. Union

For an union of two Boolean models, the resulting covariance reads:

$$\begin{aligned}\varepsilon &= \varepsilon^{(1)}\varepsilon^{(2)} \\ \gamma(h) &= \frac{1}{\varepsilon(1-\varepsilon)} \left[\bar{C}_{00}^{(1)}(h) \bar{C}_{00}^{(2)}(h) + \varepsilon^{(1)2} \bar{C}_{00}^{(2)}(h) + \varepsilon^{(2)2} \bar{C}_{00}^{(1)}(h) \right] \quad (64)\end{aligned}$$

5.2. Intersection

For an intersection of two Boolean models, the resulting covariance reads:

$$\begin{aligned}p &= p^{(1)}p^{(2)} \\ \gamma(h) &= \frac{1}{p(1-p)} \left[\bar{C}_{00}^{(1)}(h) \bar{C}_{00}^{(2)}(h) + p^{(1)2} \bar{C}_{00}^{(2)}(h) + p^{(2)2} \bar{C}_{00}^{(1)}(h) \right] \quad (65)\end{aligned}$$

5.3. Model of aggregated and isolated particles

This model corresponds to an union of two models:

- Model (a): intersection of model 1 (aggregates) with model 2 (particles in aggregates);
- Model (b): intersection of the complementary of model 1 (out of aggregates) with model 3 (particles out of aggregates).

The resulting porosities of the models read:

$$\begin{aligned}\varepsilon^{(a)} &= 1 - p^{(1)}p^{(2)} \\ \varepsilon^{(b)} &= 1 - \varepsilon^{(1)}p^{(3)} \\ \varepsilon &= \varepsilon^{(a)}\varepsilon^{(b)} = (1 - p^{(1)}p^{(2)}) (1 - p^{(3)} + p^{(1)}p^{(3)}) \quad (66)\end{aligned}$$

The corresponding covariance reads:

$$\begin{aligned}\bar{C}_{00}^{(a)}(h) &= \bar{C}_{00}^{(1)}(h) \bar{C}_{00}^{(2)}(h) + p^{(1)2} \bar{C}_{00}^{(2)}(h) + p^{(2)2} \bar{C}_{00}^{(1)}(h) \\ \bar{C}_{00}^{(b)}(h) &= \bar{C}_{00}^{(1)}(h) \bar{C}_{00}^{(3)}(h) + \varepsilon^{(1)2} \bar{C}_{00}^{(3)}(h) + p^{(3)2} \bar{C}_{00}^{(1)}(h) \\ \gamma(h) &= \frac{1}{\varepsilon(1-\varepsilon)} \left[\bar{C}_{00}^{(a)}(h) \bar{C}_{00}^{(b)}(h) + \varepsilon^{(a)2} \bar{C}_{00}^{(b)}(h) + \varepsilon^{(b)2} \bar{C}_{00}^{(a)}(h) \right] \quad (67)\end{aligned}$$

6. Relative variance of $I_{\text{proj}}(q)$ for some models

We define the relative variance $\mathcal{V}(q)$ of the SAXS intensity computed from projections by:

$$\mathcal{V}(q) = \frac{\text{Var}[I_{\text{proj}}(q)]}{E[I_{\text{proj}}(q)]^2} \quad (68)$$

This relative variance is observed to be constant over q and equal to $\frac{1}{2}$ for Boolean models of spheres with constant radius (Fig. 4 of the paper). This behavior has been observed as well for the other models considered in the paper.

6.1. Boolean model of spheres with radius following a Gamma distribution

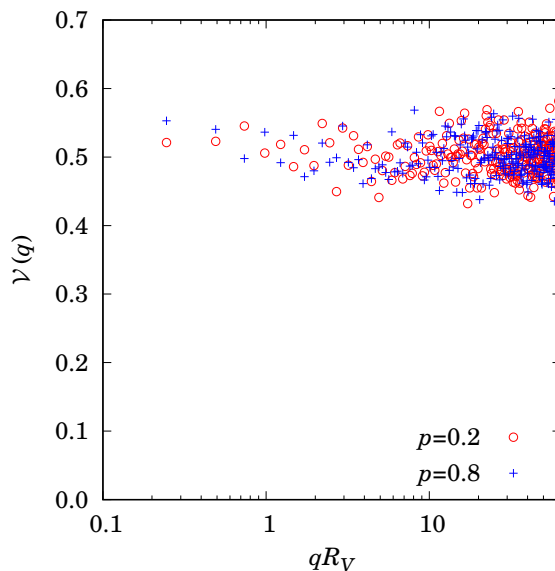


Fig. 3. Relative variance of calculated SAXS intensity from projection evaluated from 1000 realizations of Boolean models of spheres with radius following a Gamma distribution with scale parameter $b = 4$ and shape parameter $c = 2$ and volumic fraction p .

6.2. Intersection of two Boolean models of spheres

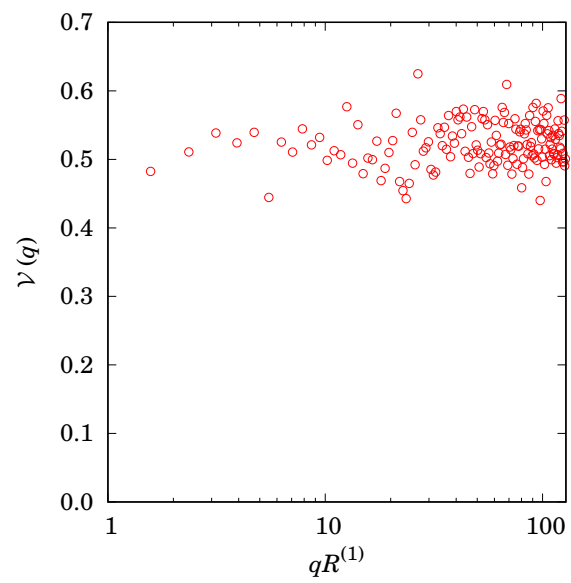


Fig. 4. Relative variance of calculated SAXS intensity from projection evaluated from 1000 realizations of an intersection of two Boolean models of spheres with constant radius. Parameters of the model are reported in Table 2 of the paper.

6.3. Cox Model

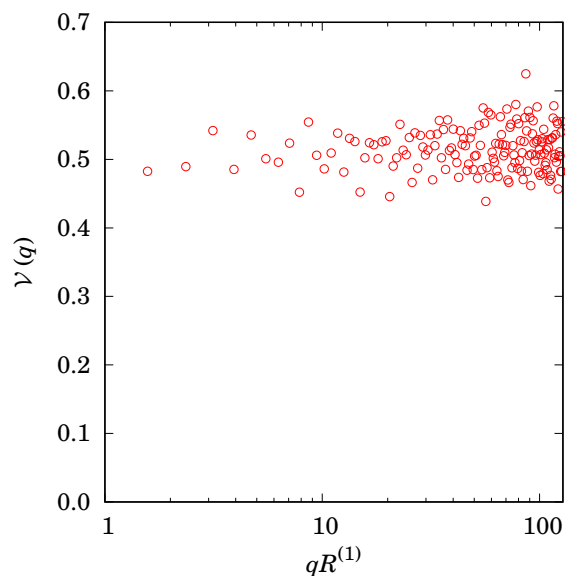


Fig. 5. Relative variance of calculated SAXS intensity from projection evaluated from 1000 realizations of a Cox Model of spheres. Parameters of the models are reported in Table 2 of the paper.

References

- Brisard, S., Chae, R. S., Bihannic, I., Michot, L., Guttman, P., Thieme, J., Schneider, G., Monteiro, P. J. & Levitz, P. (2012). *American Mineralogist*, **97**(2-3), 480–483.
- Gommes, C. J. (2018). *Microporous and Mesoporous Materials*, **257**, 62–78.
- Guinier, A., Fournet, G. & Walker, C. (1955). *Small angle scattering of X-rays*, chap. 2. New York: J. Wiley & Sons.
- Kak, A. & Slaney, M. (1988). *Principles of Computerized Tomographic Imaging*, vol. 33, chap. 3, pp. 56–57. Philadelphia: SIAM.
- Koch, K., Ohser, J. & Schladitz, K. (2003). *Advances in Applied Probability*, **35**(3), 603–613.
- Lantuejoul, C. (1991). *Journal of Microscopy*, **161**(3), 387–403.
- Levitz, P. & Tchoubar, D. (1992). *Journal de Physique I*, **2**(6), 771–790.
- Matheron, G. (1975). *Random Sets and Integral Geometry*. New York: Wiley.
- Schmidt-Rohr, K. (2007). *Journal of Applied Crystallography*, **40**(1), 16–25.
- Sonntag, U., Stoyan, D. & Hermann, H. (1981). *Physica Status Solidi (a)*, **68**(1), 281–288.